Supporting Information for

Controlled ligand distortion and its consequences for structure, symmetry, conformation and spin-state preferences of iron(II) complexes

Nicole Kroll, Kolja Theilacker, Marc Schoknecht, Dirk Baabe, Dennis Wiedemann, Martin Kaupp,

Andreas Grohmann and Gerald Hörner

Technische Universität Berlin, Institut für Chemie, Straße des 17. Juni 135, 10623 Berlin, Germany.

Technische Universität Braunschweig, Institut für Anorganische und Analytische Chemie, Hagenring 30,

38106 Braunschweig, Germany.

Table S1. Crystallographic data.

	[**1**(OTf)](OTf)	[**1**(CH$_3$CN)](BPh$_4$)$_2$	[NiL^1(ClO$_4$)] (ClO$_4$) · MeOH	[**2**(OTf)](OTf) · CH$_2$Cl$_2$	[**2**(Cl)](PF$_6$) · ¼ Et$_2$O	[NiL^2(H$_2$O)] (ClO$_4$)$_2$ · MeOH
CCDC No.	1008834	1008833	1008832	1008835	1008836	1008837
Radiation	Mo-K_α (λ = 0.71073 Å)	Cu-K_α (λ = 1.54184 Å)	Mo-K_α (λ = 0.71073 Å)	Cu-K_α (λ = 1.54184 Å)	Mo-K_α (λ = 0.71073 Å)	Mo-K_α (λ = 0.71073 Å)
Formula	C$_{25}$H$_{27}$F$_6$FeN$_5$O$_6$S$_2$	C$_{73}$H$_{70}$B$_2$FeN$_6$	C$_{24}$H$_{31}$Cl$_2$N$_5$NiO$_9$	C$_{26}$H$_{31}$Cl$_2$F$_6$FeN$_5$O$_6$S$_2$	C$_{24}$H$_{31.5}$ClF$_6$FeN$_5$O$_{0.25}$P	C$_{23}$H$_{31}$Cl$_2$NiN$_5$O$_9$
M/g · mol^{-1}	727.49	1108.82	663.15	814.43	630.31	651.14
Crystal dimensions/mm^3	0.14 × 0.14 × 0.13	0.23 × 0.09 × 0.09	0.31 × 0.07 × 0.06	0.35 × 0.31 × 0.28	0.72 × 0.21 × 0.16	0.44 × 0.11 × 0.07
Crystal description	pale yellow cube	yellow rod	light violet column	dark red block	green rod	clear light violet needle
Crystal system	monoclinic	monoclinic	monoclinic	monoclinic	triclinic	orthorhombic
Space group	$P2_1/c$	$P2_1/n$	$P2_1/c$	$P2_1/c$	$P\bar{1}$	$Pna2_1$
a/Å	11.8155(3)	12.0919(2)	9.6432(6)	13.4336(2)	8.2754(4)	16.5101(6)
b/Å	17.6019(5)	33.6364(5)	15.5442(13)	20.5689(2)	12.0926(5)	13.5280(4)
c/Å	14.8106(4)	14.6502(2)	19.6209(15)	13.4353(2)	13.8127(6)	12.2737(4)
α/°	90	90	90	90	99.414(3)	90
β/°	96.124(3)	90.4960(10)	108.042(5)	115.080(2)	90.005(4)	90
γ/°	90	90	90	90	90.983(3)	90
V/Å^3	3062.66(14)	5958.42(16)	2796.5(4)	3362.35(10)	1363.43(11)	2741.31(16)
Z	4	4	4	4	2	4
ϱ_{calc}/g · cm^{-3}	1.578	1.236	1.575	1.609	1.540	1.578
μ/mm^{-1}	0.713	2.399	0.946	6.95	0.776	0.96
F(000)	1488	2344	1376	1664	649	1352
T_{min}/T_{max}	0.92072 / 1.00000	0.6084 / 0.8131	0.91485 / 1.00000	0.32926 / 1.00000	0.85009 / 1.00000	0.81018 / 1.00000
Measured reflections/R_σ	13451 / 0.0488	46761 / 0.0435	11741 / 0.1405	30155 / 0.0200	10611 / 0.0271	11982 / 0.0376
Independent reflections/R_{int}	6006 / 0.0351	10755 / 0.0597	5481 / 0.0864	6379 / 0.0319	5338 / 0.0190	4759 / 0.0309
θ_{min}/°, θ_{max}/°	3.42 / 26.00	2.63 / 67.50	3.39 / 26.00	3.63 / 26.00	3.45 / 26.00	3.65 / 25.00
Data/restraints/parameters	6006 / 155 / 480	10755 / 0 / 739	5481 / 78 / 409	6379 / 491 / 120	5338 / 337 / 0	4759 / 399 / 59
R indices ($I > 2\sigma$)	R_1 = 0.0460	R_1 = 0.0384	R_1 = 0.0659	R_1 = 0.0339	R_1 = 0.0306	R_1 = 0.0333
	wR_2 = 0.0925	wR_2 = 0.0845	wR_2 = 0.1051	wR_2 = 0.0885	wR_2 = 0.0790	wR_2 = 0.0742
R indices (all data)	R_1 = 0.0617	R_1 = 0.0523	R_1 = 0.1188	R_1 = 0.0357	R_1 = 0.0352	R_1 = 0.0356
	wR_2 = 0.0980	wR_2 = 0.0927	wR_2 = 0.1309	wR_2 = 0.0899	wR_2 = 0.0814	wR_2 = 0.0754
GoF	S = 1.058	S = 1.035	S = 1.038	S = 1.052	S = 0.925	S = 1.057
	S' = 1.149	S' = 1.035	S' = 1.046	S' = 1.059	S' = 0.925	S' = 1.089
$\Delta\varrho_{fin}$(max/min)/e · Å^{-3}	0.362 / −0.325	0.250 / −0.303	0.989 / -0.654	0.325 / −0.888	0.341 / −0.268	0.305 / −0.332

Table S2. Selected bond lengths and angles for the nickel(II) complexes [**NiL^1**(ClO$_4$)]$^+$ and [**NiL^2**(OH$_2$)]$^{2+}$.

	[**NiL^1**(ClO$_4$)]$^+$	[**NiL^2**(OH$_2$)]$^{2+}$
bond lengths		
Ni1-N1	204.9(4)	210.2
Ni1-N4	211.5(4)	215.4
Ni1-N10	201.2(4)	210.2
Ni1-N20	206.9(4)	208.0
Ni1-N30	203.5(4)	207.9
Ni1-O	262.4(2) [a]	210.6
bond angles		
N1–Ni1–N4	78.2(1)	94.4
N1–Ni1–N30	160.8(1)	174.7
N10-Ni1-O	164.7(5)	
N4–Ni1–O		167.6
N20-Ni1-N4	154.1(2)	
N10–Ni1–N20		171.0
distortion parameters		
$\Sigma/°$	112.8	52.8
$S(O_h)$	4.03	1.96
$S(TP)$	8.00	10.46

[a] Oxygen atom O1 is disordered over two positions (O1A, O1B): Parameters involving O1A are given in the table; d(Ni1–O1B) = 272.7(2) pm; angle(N1–Ni1–O1B) = 87.4(5)°; Σ = 17.6° (O1B); $S(O_h)$ = 3.97 (O1B).

Table S3. Selected bond lengths (pm) and angles (°) from optimised structures (B3LYP-D3/def2-TZVP/COSMO(MeCN)) of the complex ions $[\mathbf{1}(X)]^{n+}$ and $[\mathbf{2}(X)]^{n+}$ in their quintet-spin states. [a]

	$[\mathbf{1}(X)]^{n+}$		$[\mathbf{2}(X)]^{n+}$	
	X = OTf	X = MeCN	X = OTf	X = MeCN
bond lengths				
Fe1-N1	220.3	221.5 *(206.7)*	224.3	223.0 *(209.8)*
Fe1-N4	228.6	229.6 *(203.8)*	226.4	225.9 *(203.8)*
Fe1-N10	215.1	216.8 *(201.1)*	214.6	217.1 *(200.6)*
Fe1-N20	228.8	229.6 *(207.3)*	216.7	218.5 *(202.0)*
Fe1-N30	214.1	216.4 *(197.7)*	218.3	220.0 *(201.5)*
Fe1-X	220.7	220.3 *(194.8)*	218.2	219.8 *(193.8)*
bond angles				
N1–Fe1–N4	72.9	72.5 *(77.8)*	90.3	90.7 *(94.4)*
N1–Fe1–N30	139.9	139.2 *(157.5)*	167.1	166.6 *(175.7)*
N4–Fe1–X	164.6	163.6 *(173.3)*	159.3	164.1 *(171.3)*
N10–Fe1–N20	156.7	153.0 *(167.0)*	162.2	162.0 *(172.1)*
distortion parameters				
$\Sigma/°$	150.9	153.4 *(90.1)*	92.5	89.5 *(51.0)*
$S(O_h)$	7.36	5.70 *(2.21)*	2.01	1.62 *(0.56)*
$S(TP)$	4.80	5.83 *(10.26)*	10.29	11.04 *(13.69)*

[a] Data in italics denote the optimised structures of the actonitrile complexes in their spin-singlet states.

Table S4. Mössbauer parameters [mm s^{-1}] obtained by least-squares fitting with doublets of Lorentzian lines. The isomer shift δ is specified relative to metallic iron at room temperature and was not corrected in terms of second order Doppler shift.

	[**1**(MeCN)](OTf)$_2$		[**1**(OTf)](OTf)		[**2**(MeCN)](OTf)$_2$		[**2**(OTf)](OTf)	
T	**20.2(1) K**	weight [a]	**20.0(1) K**	weight [a]	**20.2(1) K**	weight [a]	**20.1(1) K** [b]	weight [a]
δ	1.086(4)	77.1 %	1.138(7)	49.0 %	0.527(2)	86.7 %	0.289(22)	3.0 %
	1.196(18)	20.7 %	1.116(4)	42.2 %	1.101(32)	6.7 %	1.094(2)	86.0 %
	0.144(3π1)	2.1%	0.413(21)	8.8 %	1.057(12)	6.6 %	1.029(17)	11.1 %
ΔE_Q	2.132(10)		2.712(26)		0.345(2)		1.015(45)	
	3.027(52)		3.572(11)		2.800(110)		2.160(5)	
	1.661(62)		1.678(43)		3.468(30)		3.147(43)	
Γ_{HWHM}	0.258(8)		0.279(15)		0.151(20)		0.099(32)	
	0.293(37)		0.168(9)		0.233(77)		0.184(4)	
	0.098(48)		0.170(28)		0.123(27)		0.207(33)	
T	**100.4(2) K**	weight [a]	**100.0(1) K**	weight [a]	**99.9(1) K**	weight [a]	**100.5(1) K** [c]	weight [a]
δ	1.066(5)	79.5 %	1.138(15)	23.5 %	0.520(1)	84.7 %	0.342(30)	8.7 %
	1.220(19)	16.1 %	1.098(6)	58.7 %	1.202(31)	10.9 %	1.088(3)	82.1 %
	0.130(31)	4.4 %	0.421(42)	17.8 %	1.032(13)	4.4 %	1.028(37)	9.2 %
ΔE_Q	2.112(11)		2.335(52)		0.353(2)		1.077(61)	
	2.909(43)		3.110(18)		2.659(86)		2.123(7)	
	1.485(62)		1.356(81)		3.452(27)		3.212(94)	
Γ_{HWHM}	0.254(9)		0.215(35)		0.145(2)		0.171(37)	
	0.224(35)		0.199(12)		0.322(64)		0.176(5)	
	0.138(48)		0.284(51)		0.106(26)		0.232(70)	
T					**100.0(1) K** [d]	weight [a]	**100.6(1) K** [d]	weight [a]
δ	-		-		0.366(13)	10.2 %	0.389(27)	11.1 %
	-		-		1.097(2)	82.6 %	1.076(3)	77.2 %
	-		-		1.052(13)	7.2 %	1.090(28)	11.7 %
ΔE_Q	-		-		0.910(26)		0.883(51)	
	-		-		2.069(4)		2.033(6)	
	-		-		3.553(25)		3.062(69)	
Γ_{HWHM}	-		-		0.167(20)		0.192(36)	
	-		-		0.196(3)		0.158(4)	
	-		-		0.142(20)		0.240(53)	
T	**200.6(4) K**	weight [a]	**200.0(1) K**	weight [a]				
δ	1.021(19)	61 %	1.080(17)	29 %	-		-	
	1.128(58)	29 %	1.068(14)	42 %	-		-	
	0.194(93)	10 %	0.312(40)	29 %	-		-	
ΔE_Q	2.007(42)		2.188(95)		-		-	
	2.530(180)		2.617(52)		-		-	
	1.230(180)		1.299(77)		-		-	
Γ_{HWHM}	0.187(36)		0.167(50)		-		-	
	0.250(120)		0.153(35)		-		-	
	0.190(140)		0.240(51)		-		-	

[a] Relative spectral areas of the sub-spectra (volume fraction); fit with a ratio of the spectral areas of the low velocity peak to the high velocity peak of [b] 1.077(18) and [c] 1.101(31); [d] Measured at $T \approx 100$ K after tempering at $T = 350$ K for at least three days under reduced pressure.
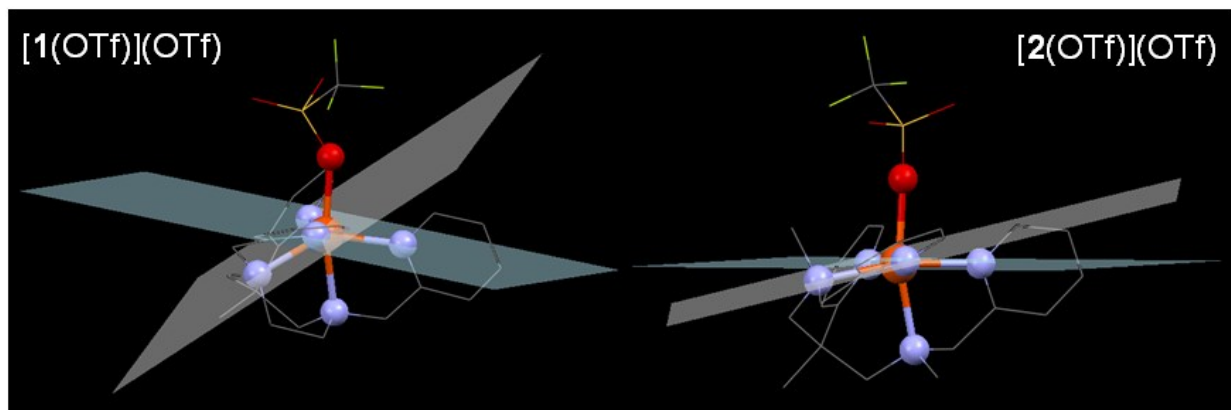
Figure S1: Distortion in the N_4 equatorial planes of the crystal structures of [**1**(OTf)](OTf) (left) and [**2**(OTf)](OTf) (right); planes defined by N(10)/N(20)/N(30) and N(1)/N(10)/N(20), respectively.
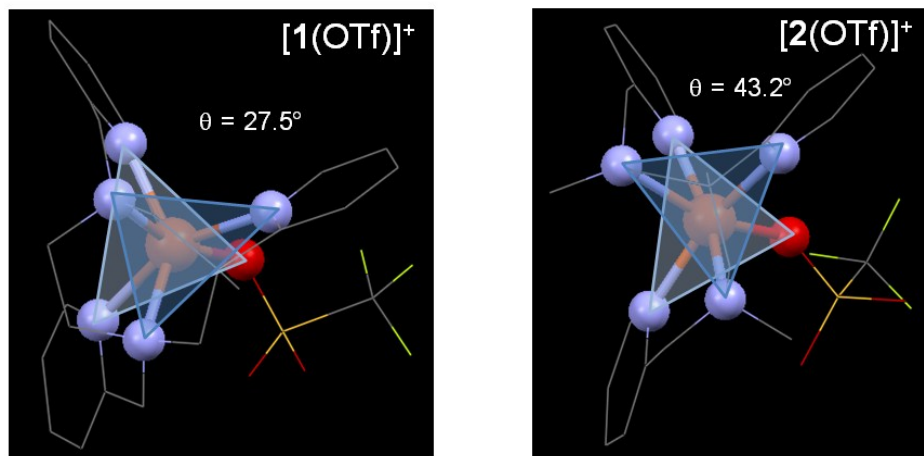

Figure S2: Optimised structures (B3LYP-D3/def2-TZVP/COSMO(MeCN)) of the complex ions [**1**(OTf)]$^+$ and [**2**(OTf)]$^+$; view along a *pseudo*-threefold axes. Average trigonal-distortion angles θ are shown.
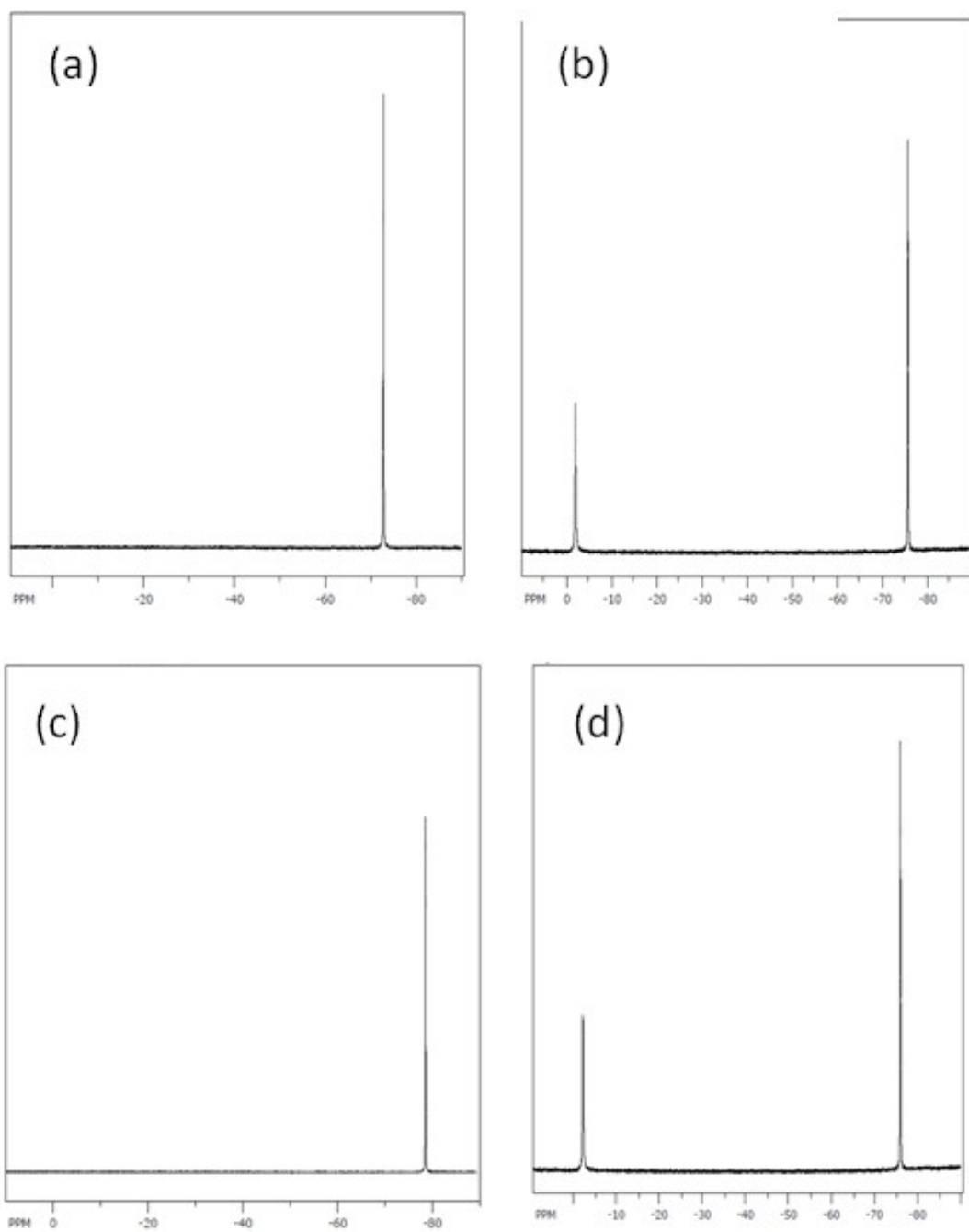
Figure S3: ^{19}F-NMR spectra (188 MHz; 295 K) of solutions of the complexes [**1**(OTf)](OTf) (a,b) and [**2**(OTf)](OTf) (c,d) in (D$_3$)-acetonitrile (a,c) and in (D$_2$)-dichloromethane (b,d).

Figure S4: Van't Hoff plots of the temperature dependence of the SCO equilibrium of [**2**(MeCN)](OTf)$_2$ in MeCN; equilibrium constants derive from measured ε_T (Figure 3c in the manuscript) as: $\boldsymbol{K = (\varepsilon(ls) - \varepsilon_T)/(\varepsilon_T - \varepsilon(hs))}$

with $\varepsilon(hs)$ =1100 L mol^{-1} cm^{-1}

black: $\varepsilon(ls)$ = 9000 L mol^{-1} cm^{-1}; red: $\varepsilon(ls)$ = 9600 L mol^{-1} cm^{-1}.

From plots of ln$K$ vs. 1/T, the thermodynamic parameters $\Delta_{SCO}S_m$ and $\Delta_{SCO}H_m$ are obtained according to: $\boldsymbol{\ln K = \Delta_{SCO}S_m/R - \Delta_{SCO}H_m\,/RT}$
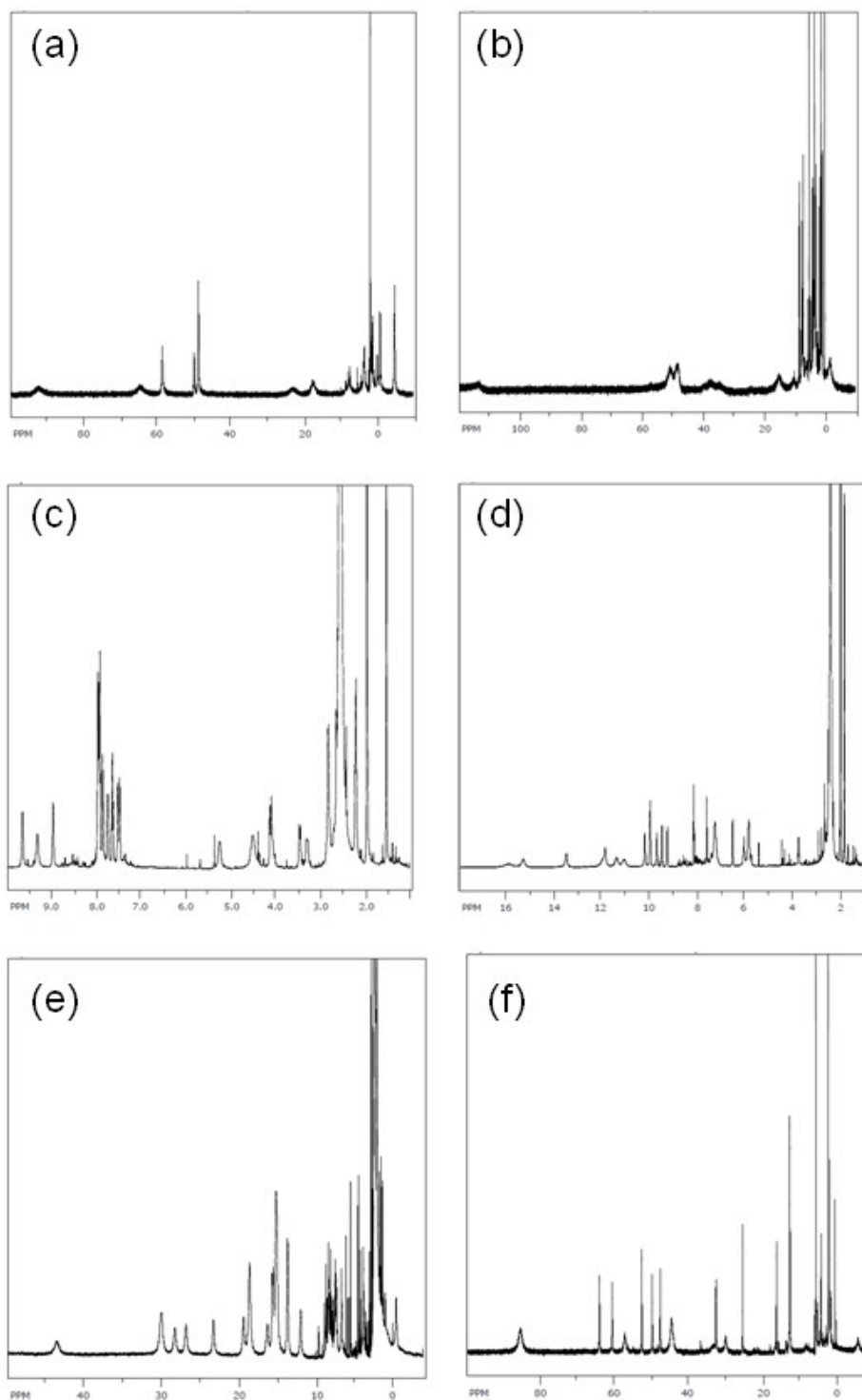
Figure S5: (a,b) ^{1}H-NMR spectra (200 MHz; 295 K) of solutions of the complex [**1**(OTf)](OTf) in [D$_3$]-acetonitrile (a) and in (D$_2$)-dichloromethane (b); (c-e) ^{1}H-NMR spectra ((D$_3$)-acetonitrile; 400 MHz) of the complex [**2**(MeCN)](OTf)$_2$ at $T = 233$ K, (c), at $T = 268$ K (d), and $T = 295$ K (e); (f) ^{1}H-NMR spectrum ((D$_2$)-dichloromethane; 200 MHz) of the complex [**2**(OTf)](OTf) at $T = 295$ K.
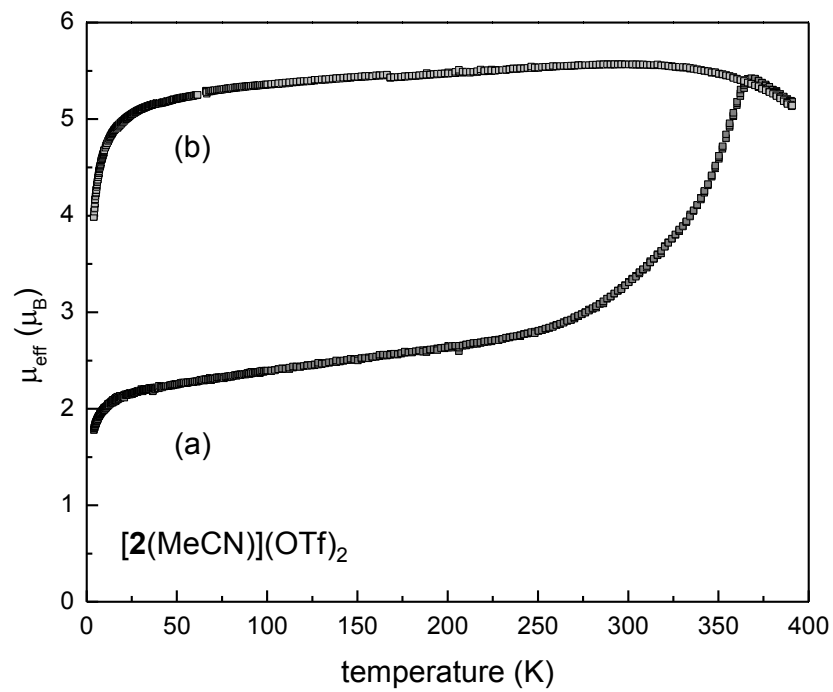
Figure S6: Temperature dependence of the effective magnetic moment of an aged powder sample of [**2**(MeCN)](OTf)$_2$; (a) 1st heating cycle; (b) 2nd heating cycle.